Joule

Article

Techno-economic analysis and life cycle assessment for the catalytic hydrogenolysis and hydrocracking of polyethylene

Graphical abstract

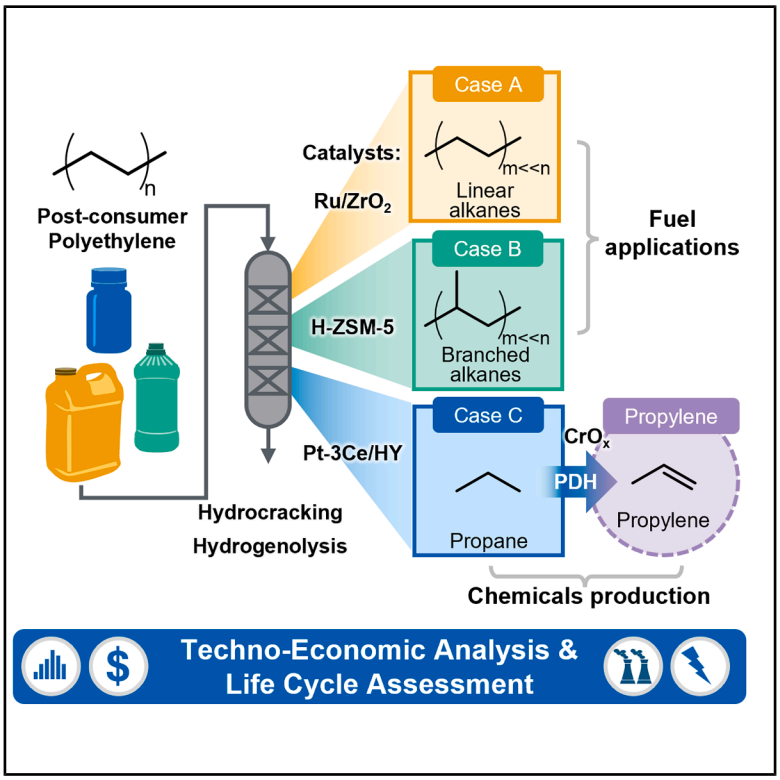

Highlights

- TEA and LCA compare PE hydrogenolysis and hydrocracking across different products
- Branched alkanes and propylene from waste PE near cost parity with fossil products
- Hydrocracking-derived propylene shows near-parity GHGs due to high yield, low H_2 use
- Feedstock cost, product yield, and plant size are key drivers of process viability

Authors

Geetanjali Yadav, Taylor Uekert, Jason S. DesVeaux, ..., Nicholas Carlson, Yuriy Román-Leshkov, Gregg T. Beckham

Correspondence

yroman@mit.edu (Y.R.-L.), gregg.beckham@nlr.gov (G.T.B.)

In brief

Post-consumer polyethylene can be selectively transformed into fuels and chemicals through catalyst-directed hydrocracking and hydrogenolysis. By tuning catalyst functionality, linear and branched liquid alkanes for fuel applications or propane for downstream propylene production can be preferentially generated. Techno-economic analyses and life-cycle assessments reveal how product selectivity governs cost and carbon intensity, providing actionable guidance for designing economically viable, low-emissions pathways for plastic waste conversion.

Yadav et al., 2026, Joule *10*, 102384
July 15, 2026
https://doi.org/10.1016/j.joule.2026.102384

CellPress

Please cite this article in press as: Yadav et al., Techno-economic analysis and life cycle assessment for the catalytic hydrogenolysis and hydrocracking of polyethylene, Joule (2026), https://doi.org/10.1016/j.joule.2026.102384

Joule

CellPress

Article

Techno-economic analysis and life cycle assessment for the catalytic hydrogenolysis and hydrocracking of polyethylene

Geetanjali Yadav,[1,2] Taylor Uekert,[1,3] Jason S. DesVeaux,[1,2] Elisabeth C. Van Roijen,[1,2] Julie E. Rorrer,[1,4,5] Anna E. Brenner,[4] Griffin Drake,[4] Guido Zichittella,[4] Nicholas Carlson,[2] Yuriy Román-Leshkov,[4,*] and Gregg T. Beckham[1,6,7,*]

[1]BOTTLE Consortium, Golden, CO 80401, USA
[2]Catalytic Carbon Transformation and Scale-up Center, National Laboratory of the Rockies, Golden, CO 80401, USA
[3]Strategic Energy Analysis Center, National Laboratory of the Rockies, Golden, CO 80401, USA
[4]Department of Chemical Engineering, Massachusetts Institute of Technology, Cambridge, MA 02142, USA
[5]Department of Chemical Engineering, University of Washington, Seattle, WA 98195, USA
[6]Renewable Resources and Enabling Sciences Center, National Laboratory of the Rockies, Golden, CO 80401, USA
[7]Lead contact
*Correspondence: yroman@mit.edu (Y.R.-L.), gregg.beckham@nlr.gov (G.T.B.)
https://doi.org/10.1016/j.joule.2026.102384

CONTEXT & SCALE Heterogeneous catalysts can be used in the presence of hydrogen gas to break down polyolefin waste into hydrocarbon products, and the research community has made major advancements in this field in the last several years with new catalysts and reactors that enable selectivity toward valuable products. Despite considerable progress, the economic and environmental impacts of catalytic hydrogenolysis, a chemical recycling method, remain insufficiently explored. In this work, we use process modeling, techno-economic analysis, and life-cycle assessment to study three distinct catalytic hydrogenolysis processes to produce linear hydrocarbons, branched hydrocarbons, and light olefins. Our work shows that while these options are technically feasible, their economic and environmental impacts are either less favorable or equivalent to primary production. These results can help the research community prioritize research questions and target the most impactful challenges in catalyst design, reaction conditions, and process development.

SUMMARY

Catalytic hydrogenolysis and hydrocracking are promising technologies for the conversion of polyolefin waste into hydrocarbons. To explore the economic and environmental viability of these approaches, we conducted techno-economic analysis and life cycle assessment of polyethylene hydrogenolysis and hydrocracking processes that produce fuel-range products or olefins, respectively. Relative to primary production, the minimum selling price (MSP) of alkanes for linear-chain naphtha was estimated to be 1.8-fold higher, whereas branched-chain naphtha and propylene were shown to be cost competitive. Environmental impacts showed similar trends across scenarios, with propylene production by hydrocracking exhibiting greenhouse gas emissions comparable with conventional propylene due to relatively low hydrogen demand and high yield. Together, these results suggest that innovations in catalysis and reaction engineering will be required to make viable products that are scale matched with today's plastics, such as light olefins for closed-loop recycling.

INTRODUCTION

Polyethylene (PE) is the most abundantly produced polymer globally,[1,2] with applications in myriad consumer goods, industrial products, and packaging. In the United States (US) alone, recycling rates for high-density PE (HDPE) and low-density PE/linear low-density PE (LDPE/LLDPE) in 2019 were 10% and 2%, respectively. The remainder was predominantly landfilled, contributing to economic losses of ~$7.2 billion.[3] Furthermore, the production of the ethylene monomer for PE manufacturing is estimated to consume ~2,000 PJ of energy per year, which is over 25% of US annual energy demand for organic petrochemical production.[4]

In light of global plastic waste pollution,[5,6] chemical recycling has gained traction as a means to increase polymer circularity.[7–15] Unlike polyesters, which contain readily cleavable

Please cite this article in press as: Yadav et al., Techno-economic analysis and life cycle assessment for the catalytic hydrogenolysis and hydrocracking of polyethylene, Joule (2026), https://doi.org/10.1016/j.joule.2026.102384

C–O bonds, polyolefins such as PE and polypropylene are connected by strong C–C bonds that are challenging to depolymerize selectively to monomer. Pyrolysis and gasification can deconstruct polyolefin feedstocks into hydrocarbon mixtures and syngas (H_2, CO, and CO_2), respectively, but their energy intensities can be 1.5–2.5 times higher than those of primary manufacturing.[16,17]

Given the challenges with pyrolysis and gasification, many efforts are underway to develop lower-temperature routes for polyolefin chemical recycling.[14,18–21] Notably, catalytic hydrogenolysis and hydrocracking cleave C–C bonds in polyolefins using H_2 to produce alkanes, with product distributions dependent on the catalytic chemistry. Hydrogenolysis of polyolefins occurs over supported noble (Ru, Pt) and non-noble (Ni, Co) metallic catalysts at ~200°C–300°C and ~1–70 bar H_2, typically yielding linear, lubricant-range waxes, and fuel-range hydrocarbon liquids with methane as the major side product.[21–46] Methane is a low-value product that consumes a significant amount of H_2, and as a result, many strategies have been pursued to reduce methane formation in hydrogenolysis, including altering particle size,[32–35,47,48] catalyst architecture,[24,34,39,49–51] reactor configuration,[45,52] catalyst composition,[43,53] temperature, hydrogen pressure, and more. As another strategy to minimize methane formation, various catalysts have been developed that combine metallic species with Brønsted-acidic supports or co-catalysts, enabling conversion of polyolefins through a bifunctional hydrocracking mechanism.[41,54–67] In this reaction, which occurs under slightly higher temperatures relative to hydrogenolysis (225°C–375°C, ~1–100 bar H_2), metal and acid sites work cooperatively to promote dehydrogenation/hydrogenation and carbocation-mediated isomerization and β-scission, respectively.[68] Consequently, hydrocracking products have a greater degree of branching and often a reduced selectivity to methane. The average carbon number of the product distribution depends strongly on the catalyst metal-acid balance,[55,57] with increasing acid activity leading to more cracking events and lighter products, resulting in propane- and butane-rich product distributions in metal-free, high-activity cracking.[57] Recent hydrocracking studies have shown that zeolite mesoporosity, acidity, and crystallinity can be manipulated to control the activity and product distribution.[56,62,69,70] Taken together, studies to date broadly indicate that it is possible to produce a distribution of alkanes that could potentially be integrated into petrochemical refineries, or to produce a narrow range of C3–C6 compounds that could be dehydrogenated to olefins for new polymer production.

For reductive strategies to become viable for waste conversion, it is important to understand which products are optimal targets and to identify the process variables that most significantly affect the process economics and environmental impacts.[71,72] To that end, we modeled three reductive PE conversion pathways to examine very different product streams: linear straight-run naphtha, highly branched alkanes, and light olefins, then conducted techno-economic analysis (TEA) and life cycle assessment (LCA) for each process. These cases were selected as archetypes representing distinct mechanistic classes (hydrogenolysis, bifunctional hydrocracking, and acid cracking). Each system we selected yields a fundamentally different carbon-number distribution and degree of branching: (1) Ru/ZrO_2 produces mainly linear alkanes via C–C bond scission on metal sites, (2) Pt-3Ce/HY yields a mixture of linear and highly branched alkanes through sequential hydrogenation-dehydrogenation and acid cracking steps, and (3) H-ZSM-5 generates light gases via protolytic β-scission. To ensure accurate representation of the literature, we surveyed reports for catalysts that achieve the highest experimental yields within each class under realistic conditions to compare the "best case" of hydrogenolysis, bifunctional hydrocracking, and acid cracking. For the case in which the process model targets branched alkane products, we also modeled how this product stream could be integrated into an existing refinery to assess its economic viability as a gasoline blendstock across a range of economic scenarios. Furthermore, a model was developed that incorporated alkane dehydrogenation to olefins to illustrate an approach for closed-loop chemical recycling. Overall, this study identifies the key cost, greenhouse gas (GHG) emissions, and energy use drivers in PE hydrogenolysis and hydrocracking.

Process model construction

Process models were developed in Aspen Plus V14. The stream mass flows for the two principal product scenarios modeled in this study—alkanes for fuels (cases A and B) and alkanes for chemicals (case C)—are presented in Figure 1. The plastic recycling facility was modeled at a scale of 240 metric tons per day (TPD) of post-consumer PE (~79,200 metric tons per year), which is the average size of a materials recovery facility (MRF) in the US (Figure S1).[3] The product yields for this 240 TPD conceptual facility were based on laboratory-scale experimental results.[33,57,67]

A process flow diagram (PFD) for the "alkanes for fuel" product is presented in Figure 2, representing both cases A and B, and noting that the feedstock pretreatment and hydrogenolysis areas (green and yellow, respectively, in Figure 2) are identical to the unit operations for "alkanes to chemicals" in case C (*vide infra*). Detailed PFDs along with stream composition data and unit operation information for all cases are provided in Figures S3–S8. We assumed the same PE feedstock in all three models (Figure 1), specifically, clean, post-consumer-grade A LDPE bales (totaling 95% clear or natural PE container and film), delivered from an MRF at $0.30/kg.[73] The historical prices of major polyolefin waste streams, including LDPE films (grade A and B), polypropylene, and HDPE (rigid, natural, and colored), are provided in Figure S1 to illustrate the variation in feedstock prices over time. Prior to depolymerization, feedstock pretreatment was modeled as debaling and melting. Feedstock is first debaled and converted to flakes (60 mm) using custom-designed PE debalers (2 parallel lines, each with a 120 TPD capacity) powered by electric motors (211 kWh/line).[74] Next, the preheater unit melts the PE flakes (melting temperature, T_m~112°C) using heat from the hydrocracker effluent, generating a melt flow stream.[75]

After pretreatment, the melted plastic feedstock undergoes depolymerization in a catalytic fixed-bed reactor (modeled as a hydrocracker, Figure 1) with liquid downflow at a reaction temperature (T_{rxn}) of 240°C–375°C and a hydrogen reaction pressure (P_{rxn}) of 40–100 bar. Before entering the reactor, the makeup and recycled H_2 gases are compressed to the

Please cite this article in press as: Yadav et al., Techno-economic analysis and life cycle assessment for the catalytic hydrogenolysis and hydrocracking of polyethylene, Joule (2026), https://doi.org/10.1016/j.joule.2026.102384

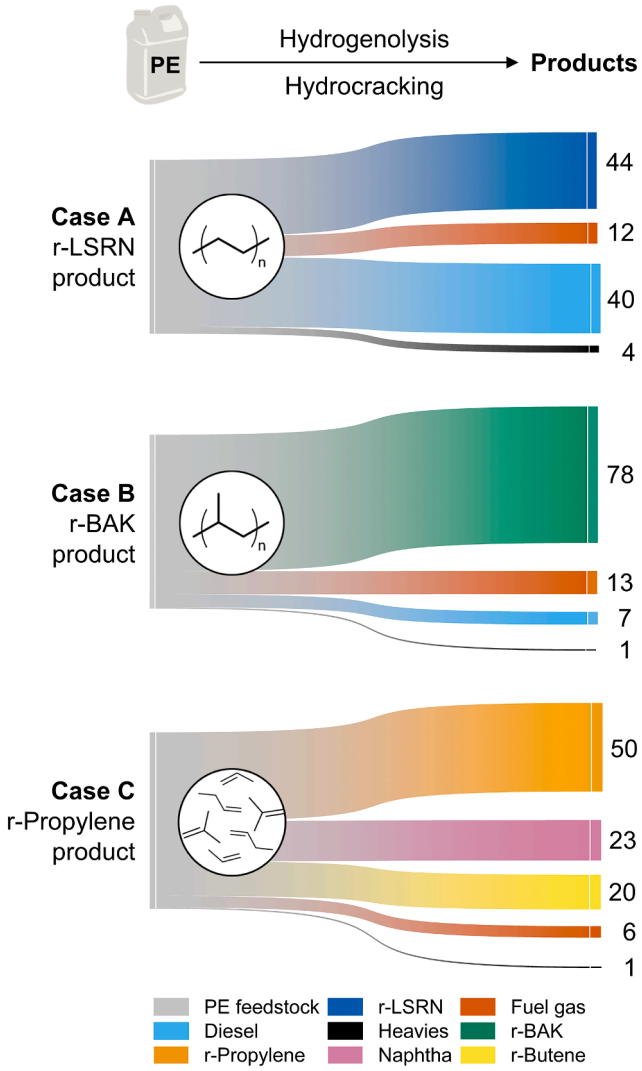

Figure 1. Sankey diagrams for the 3 cases for polyolefin hydrogenolysis examined in this study

Alkanes for fuel product:

(A) Case A: r-linear straight-run naphtha (LSRN) product. The principal product consists of low-molar-mass, linear straight-run alkanes, along with co-products of fuel gas, diesel, and heavies. The fuel gas stream, which contains C1-C3 hydrocarbons, is converted to electricity as a co-product in the base case.

(B) Case B: r-branched alkanes (r-BAK) product. The liquid product consists of branched alkane products. Co-products of fuel gas, diesel, and heavies are recovered as shown.

Alkanes for chemical products:

(C) Case C: r-propylene product. Here, the main product is propylene, followed by co-products of naphtha, r-butene, fuel gas, and heavies.

conditions of the depolymerization reactor. A stochiometric excess of cold H_2 gas is supplied as a quench between the catalyst beds inside the reactor to maintain isothermal conditions by dissipating the heat generated from the depolymerization reactions,[76] ensuring that the temperature rise remains within an operating range of $T_{rxn} \pm 30^{\circ}C$ (rising over this range from the inlet to the outlet). For simplicity, it is assumed that no internal concentration gradients occur within the catalyst, so the effectiveness factor is taken as 1;[77] potential mass transfer limitations in industrial systems are acknowledged and their effects explored through sensitivity analysis of product yields (*vide infra*).

In the hydrocracker, the catalysts in all cases are modeled to be used for 2 years, during which their activity gradually decreases with increasing time-on-stream. However, the model assumes that dehydrogenation activity is maintained at a constant level throughout the catalyst lifespan, assuming that product selectivity remains unchanged. We acknowledge that additives and contaminants in post-consumer plastics may cause catalyst deactivation; as described below, this was addressed through sensitivity analysis of both catalyst replacement time (1–3 years) and product yields. Further details are provided in the supplemental methods section. The catalyst cost was estimated using CatCost (Tables S1–S3).[78]

The effluent from the reactor passes through heat exchangers to a high-pressure separator operating at 28 bar. Here, H_2 gas is separated from the top of the column, while liquids are recovered from the bottom. A pressure swing adsorption unit operating at 20 bar recovers 85% of the hydrogen from the incoming gaseous stream to a purity of 99%.[79] The remaining gases are depressurized to 2 bar and either combusted and sold as electricity (cases A and B) or sent to the light gaseous alkanes recovery process section (case C, *vide infra*), depending on the product scenario. A steam cycle and turbine are used to produce electricity that is sold to the grid after meeting all the electricity needs of the plant. The liquid stream from the bottom of the high-pressure separator is sent to a low-pressure separator (~1 bar) to remove additional gases. Finally, the liquid stream, containing *n*-alkanes, *iso*-alkanes, and other case-dependent, naphtha-range hydrocarbons, is sent for distillation. In the distillation column, the low-molar-mass liquid alkanes (C5–C15) are extracted as the overhead fraction, while the heavy naphtha (>C15) boiling-range streams are removed as the bottom liquid product. All unreacted feedstock from the fractionator bottom is sent back to the reactor as a recycle stream for further depolymerization, and the solids are sent to the waste treatment section. In this way, an overall 100% conversion of feedstock to products is modeled.

Material and energy balances from the process models for each case were used to estimate the equipment size and the corresponding capital investment for the hydrogenolysis facility. Information on raw materials, utilities, labor, maintenance costs, and other factors was used to estimate the annual operating expenses. A discounted cash flow analysis approach (financial parameters in Table S4) was applied to calculate the minimum selling price (MSP) of the primary products produced by this facility on a 2024 US dollar cost basis, with co-products such as fuel gas, electricity, diesel, naphtha, and others sold at their respective 5-year average market prices.[80]

The life cycle impacts were determined using material and energy balances from the process models (Tables S5–S7), ecoinvent v3.9.1 background data (allocation, cut-off by classification - unit, US-specific inventories when available, global inventories otherwise),[81] Brightway v2.9.7 software, and the Intergovernmental Panel on Climate Change (IPCC) 2021 and

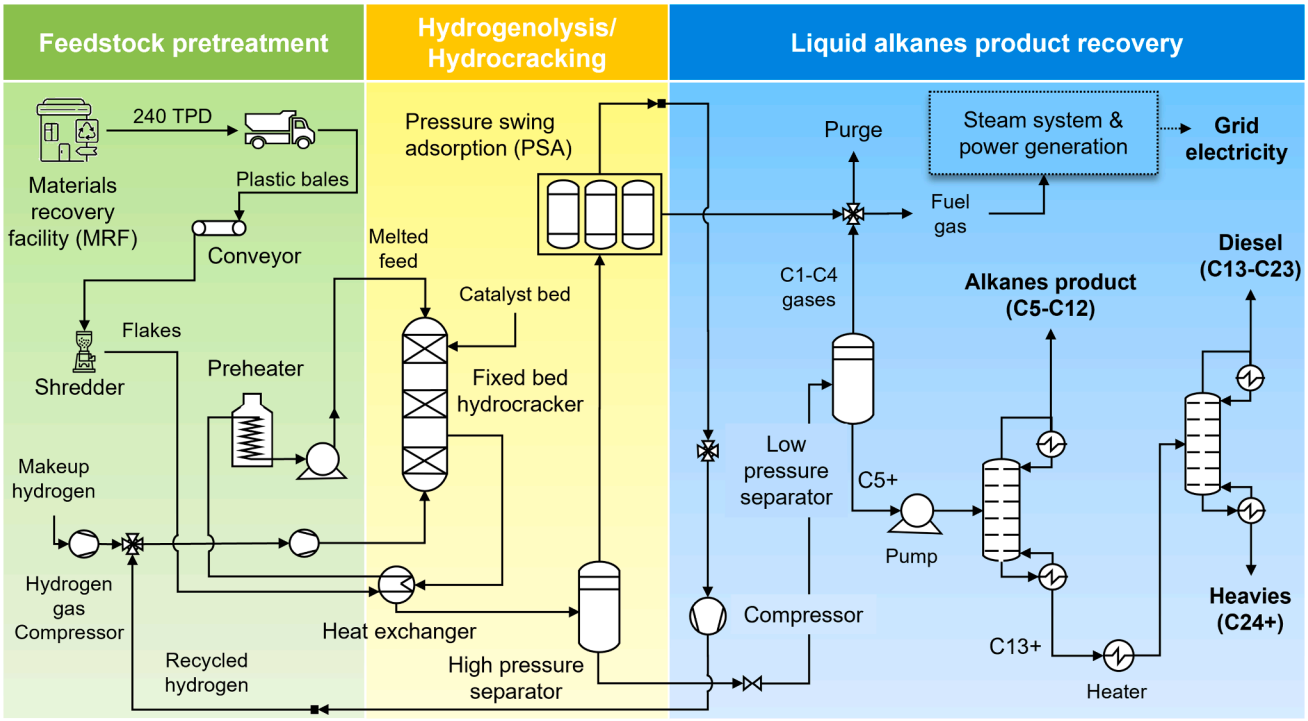

Figure 2. PFD for alkanes for fuel cases (cases A and B)

Simplified PFD of the polyolefin hydrogenolysis or hydrocracking process, divided into three sections. Feedstock pretreatment: polyolefin bales are debaled, flaked, and melted. Hydrogenolysis/hydrocracking: polymer flakes are catalytically depolymerized with H_2 gas to produce liquid alkanes in the presence of a catalyst. Liquid alkanes product recovery: the reactor effluent is cooled and separated from the gaseous stream in a pressure swing adsorption unit to recover a H_2-rich gas stream, while liquids are recovered through fractionation. Detailed PFDs are provided in Figures S3–S7.

ReCiPe Hierarchist midpoint impact assessment methods.[82,83] The environmental metrics of products produced via hydrogenolysis were compared with conventional fossil-based routes for the same products. Hydrogenolysis was assessed "cradle-to-gate," from curbside collection of mixed recyclables (life cycle inventory sourced from the literature[84]) through to the final hydrogenolysis product(s). The manufacturing of the plastic feedstock and the use of the produced chemicals were not included in this scope. Co-products were assumed to displace conventional production of the materials or energy, and were given corresponding credits according to the system expansion approach. The sensitivity of co-product handling was also tested by comparing it with the mass allocation approach; for all metrics except fossil fuel depletion, the mass allocation results fall within the uncertainty range of the system expansion results. Standard deviations were estimated using the built-in ecoinvent uncertainty data and Monte Carlo analysis.[85]

RESULTS

Alkanes for fuels

We modeled two alkanes for fuel product scenarios: hydrogenolysis to a linear alkane product (case A: r-LSRN [linear straight-run naphtha]) and to a branched alkane product (case B: r-BAK). The PFD is the same in both cases, as shown in Figure 2.

Case A: r-LSRN product

Here, we modeled linear alkanes as the primary product with a chain length of C5–C12, similar to a typical virgin linear straight-run naphtha (v-LSRN) stream obtained by distilling crude oil in a refinery. The catalyst, 5 wt % Ru/ZrO_2,[33] has been reported in laboratory-scale batch reactions to catalyze the hydrogenolysis of PE to linear alkane products at 240°C and 60 bar H_2, resulting in total liquid (C5–C22) yields up to 85%, with C5–C12 fractions accounting for 44%. The remaining products consist of a wax co-product and a low-molar-mass gaseous hydrocarbon stream (C1–C4), referred to as fuel gas. The reaction conditions (T_{rxn} = 240°C and P_{rxn} = 60 bar), yields, and residence time from the previous report are directly used as the input to our reactor, with the C5–C12 fraction as the r-LSRN product and other hydrocarbon liquids as co-products. Fuel gas is combusted on-site to generate electricity through a conventional steam cycle, for which credits are included in the TEA and LCA at the 5-year average market price and the environmental impact of the US average electricity grid.[80]

For case A, the total capital investment (TCI) for a plant processing 240 TPD of PE is $136 million (M), as shown in Figure 3A, with the highest contribution from the hydrogenolysis section, followed by the outside battery limits section (OSBL, which includes auxiliary equipment such as storage tanks, power generation, and wastewater treatment). The total annual operating expense for this plant is $53 M (Figure S9). The MSP

Please cite this article in press as: Yadav et al., Techno-economic analysis and life cycle assessment for the catalytic hydrogenolysis and hydrocracking of polyethylene, Joule (2026), https://doi.org/10.1016/j.joule.2026.102384

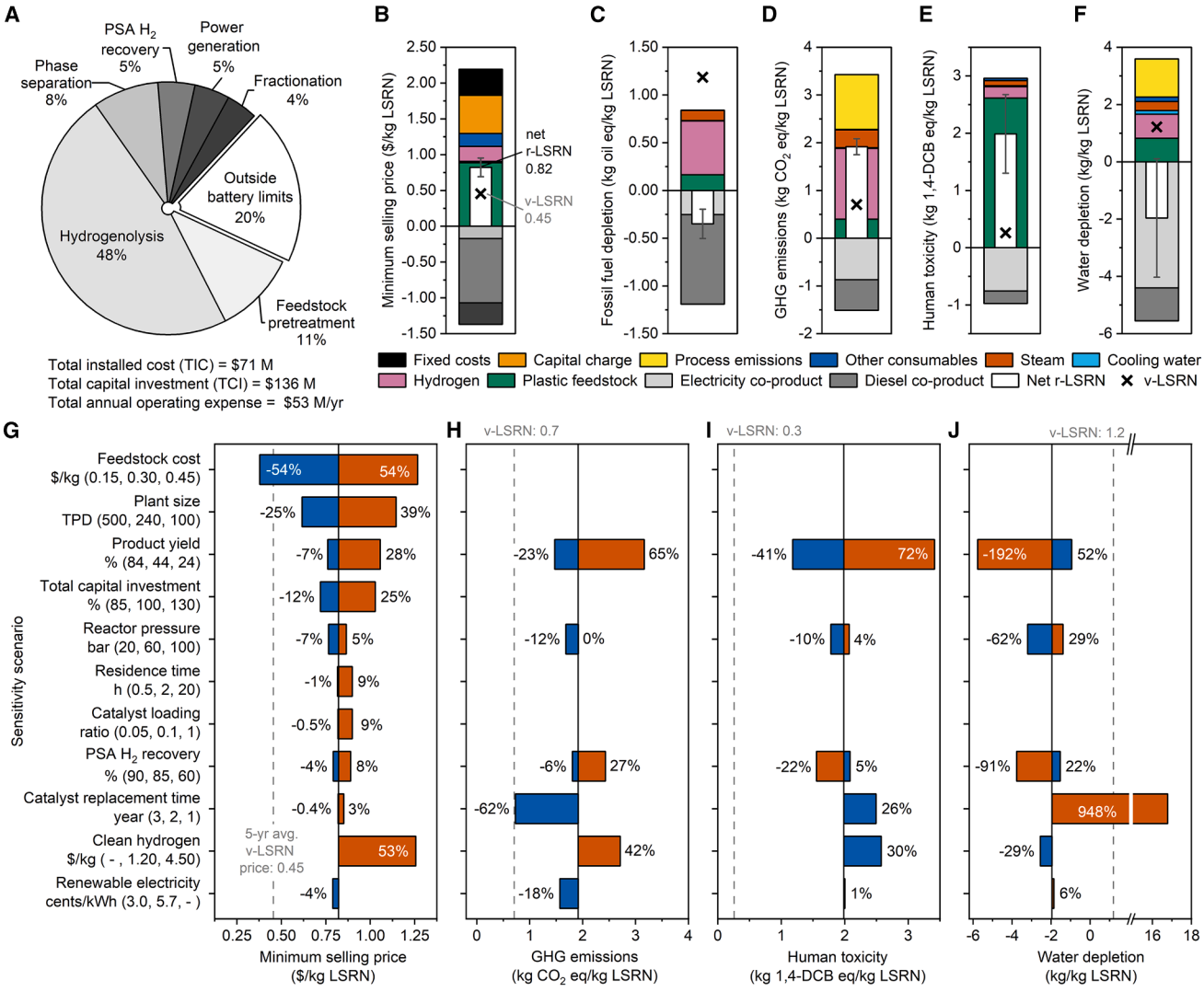

Figure 3. TEA, LCA, and sensitivity analysis results for case A (r-LSRN product)

(A) Capital cost breakdown by area for each process section for case A, with TCI of $136 M. The total installed capital (TIC) is split into different steps of the recycling process, including OSBL, which is assumed to be 25% of the battery limit investment.

(B) The MSP of the product. The net value is shown as a white bar with the contribution breakdown shown behind the net value as colored segments. The 5-year average market price for v-LSRN is shown for reference as a black "x". Error bars showing the standard deviation were estimated from a Monte Carlo analysis with 10,000 runs.

(C–F) Results for (C) fossil fuel depletion, (D) GHG emissions, (E) human toxicity, and (F) water depletion for the process. The net value and contributions are shown in a similar manner to the MSP.

(G–J) The effect of sensitivity cases on (G) MSP, (H) GHG emissions, (I) human toxicity, and (J) water depletion. Blue and orange bars indicate the optimistic and pessimistic sensitivity cases, respectively, corresponding to the values in the *y*-axis labels. LCA calculations were conducted with IPCC 2021 and ReCiPe methodologies, Brightway software, and ecoinvent 3.9.1 background data. Data for this figure are available in Tables S8–S18 for the TEA and Tables S17–S21 for the LCA.

for r-LSRN in the base case is estimated to be $0.82/kg, which is 1.8 times that of v-LSRN (Figure 3B). Feedstock cost is the major economic driver, followed by the capital charge, fixed costs, and the cost of H_2. A summary of the process and economic results—including detailed information on the specific unit operations, capital and operating cost requirements for each process section, a breakdown of the MSP, and the rationale and results of the TEA sensitivity analysis—is provided in Tables S8–S18.

Production of r-LSRN is estimated to have lower freshwater eutrophication, fossil fuel depletion, ionizing radiation, land use, metal depletion, ozone depletion, particulate matter formation, photo-oxidant formation, terrestrial acidification, and water depletion than v-LSRN (Figures 3C–3F; Tables S19 and S20). This is primarily due to credits received for electricity co-generation (1.8 kWh generated per kg of r-LSRN), which is assumed to displace the current US grid comprising 37% natural gas, 19%

Please cite this article in press as: Yadav et al., Techno-economic analysis and life cycle assessment for the catalytic hydrogenolysis and hydrocracking of polyethylene, Joule (2026), https://doi.org/10.1016/j.joule.2026.102384

coal, 18% nuclear, 11% wind, 6% solar, and 9% other,[86] and emitting 0.47 kg CO_2e/kWh. However, GHG emissions, ecotoxicity, marine eutrophication, and human toxicity of r-LSRN are estimated to be 3 times, 43%, 87%, and 8 times higher, respectively, than v-LSRN. Across all life cycle metrics, plastic collection and sortation contribute 12%–96%, H_2 accounts for 1%–67%, and steam contributes 2%–37%. The impacts of the plastic feedstock are related to electricity use for sorting equipment (0.07 kWh/kg feedstock), landfilling of contaminants during the sorting process (0.1 kg/kg feedstock), and transporting the feedstock by diesel-powered trucks between collection, sorting, and hydrogenolysis facilities (a total of 700 km).[87] Hydrogen (0.13 kg/kg r-LSRN) was assumed to be generated by steam methane reforming, which accounts for most of current US production[88] and emits 8–11 kg CO_2e/kg H_2 as well as criteria air pollutants such as nitrogen oxides, particulate matter, and volatile organic compounds.[89,90] The impacts of steam (1.1 kg/kg r-LSRN) are linked to its generation from natural gas and other fossil fuels. Other consumables—which include the hydrogenolysis catalyst—only contribute significantly to metal depletion (24%) and land use (11%) due to zircon mining and processing into ZrO_2. The release of 1.1 kg CO_2 from combustion of the fuel co-product to generate electricity also accounts for 34% of GHG emissions.

Univariate sensitivity analysis was performed to identify the key parameters that influence the economic and environmental viability of PE hydrogenolysis to r-LSRN (Figures 3G–3J; Tables S18 and S21). In the r-LSRN base case, feedstock cost exhibited the highest contribution to MSP. Most of the feedstock cost arises from the collection and sortation of PE into bales at MRFs. Market reports indicate that the average price of mixed LDPE Grade A bales ranged from $0.14 to $0.48/kg in the US from 2016 to 2024 (Figure S1).[73] As shown in the MSP tornado plot (Figure 3G), a feedstock cost of $0.15/kg allows for cost parity with v-LSRN. Next, the impact of plant size variation on MSP was assessed, assuming an abundant feedstock supply could be obtained at the same price. Doubling plant capacity to 500 TPD reduces the MSP by 25% and environmental impacts by 22%–28%, due to economies of scale that maximize the efficiency of heat integration and utility usage.

Among technical parameters, principal product yield is most impactful on the MSP (Figure 3G). Several other variables, including catalyst loading and replacement time, residence time, and hydrogenolysis reactor pressure, exhibit marginal effects on the MSP. The hydrogenolysis process and product separation occur mostly under higher pressure conditions, which helps reduce compression requirements when recycling H_2 gas to the reactor. As a result of this design, a change in reactor pressure has a negligible impact on the economics across the range explored. Nevertheless, reducing H_2 pressure does slightly increase the amount of electricity that can be treated as a co-product rather than used to pressurize the hydrogenolysis reactor, facilitating minor improvements (>10%) across environmental impacts. Lastly, increased H_2 recovery (90%) can reduce MSP by 4% compared with the base case, whereas a lower recovery (60%) can increase MSP by up to 8%. Given the higher contribution of H_2 to r-LSRN impacts in comparison with MSP, adjusting H_2 use or source represents a significant opportunity for environmental optimization. Increasing H_2 recovery relative to the base-case assumptions reduces GHG emissions by 6%, but, interestingly, lowers the performance of other metrics (e.g., toxicity or water use) because the quantity of H_2 lost is counterbalanced by the quantity of electricity that can be generated from that loss. For example, 60% H_2 recovery uses 0.24 kg H_2/kg r-LSRN but generates 3.3 kWh, whereas 90% H_2 recovery uses 0.11 kg H_2/kg r-LSRN but generates 1.5 kWh. Additional sensitivity cases were explored, including those for discount rate, income tax rate, catalyst cost, variable operating expenses, and the results are provided in Table S18.

Lastly, economy-wide scenarios were considered in which H_2 from steam methane reforming is displaced by clean H_2 produced from water electrolysis coupled with renewable electricity, alternative sources of steam are used (produced from biomass), and the current US grid mix is replaced by a mostly renewable electricity grid comprising 43% wind, 32% photovoltaics, 21% nuclear, 5% hydropower, 5% natural gas, 1% geothermal, and 2% other.[91] The use of clean H_2 (production cost of $4.50/kg)[92] and decarbonized steam ($5.39/kg)[93] resulted in increases in the MSP of 53% and 4%, respectively. In contrast, the shift to a renewable electricity ($0.03/kWh)[94] grid reduced the MSP by 5%. Given that H_2 and steam are key contributors to r-LSRN impacts, switching to alternative production methods could reduce the GHG emissions of hydrogenolysis by 62% and 18%, respectively. A trade-off is that the clean H_2 would increase human toxicity and water use due to the high electricity requirements of water electrolysis (55 kWh/kg H_2). Interestingly, renewable electricity would not benefit hydrogenolysis, as the credits received for electricity co-generation would decrease.

Case B: r-BAK product

In this case, a bifunctional hydrocracking process is utilized to produce branched alkanes with characteristics similar to v-BAK from a petroleum refinery. The modeled hydrocracking process, from Zhao et al.,[67] was reported to operate in batch reactors at T_{rxn} = 280°C and P_{rxn} = 40 bar H_2 (20 bar H_2 filling pressure, scaled by reaction temperature), resulting in a total liquid alkane yield of 85 wt % in the C5–C14 range (including both linear and branched isomers), with a narrow selectivity toward branched alkanes. This is accomplished using a platinum-zeolite HY catalyst with a cerium promoter (0.5 wt % Pt, Si/Al = 2.25, 3 wt % Ce) denoted Pt-3Ce/HY, in which the authors reported that Pt facilitated de/hydrogenation, Ce improved dispersion and stability, and HY zeolite performed hydrocracking and hydroisomerization.[67] As in case A, these conditions and results are directly incorporated into the process model, with the branched C5–C12 fraction (71 wt %) as the r-BAK product.

The TCI of the plant is $108 M, with contributions similar to those discussed in the r-LSRN case (Figure 4A). The facility would require $51 M in annual operating expenses. A detailed breakdown of annual operating expenses is shown in Figure S10, which is dominated by feedstock costs, with H_2 consumption being the other major driver in the depolymerization section, and recovery of co-products largely offsets these costs. Overall, the r-BAK MSP is more economically favorable than case A, with the MSP of r-BAK being 7% lower than v-BAK (Figure 4B). More details on the economic summary and MSP with TEA and LCA sensitivities are provided in Tables S22–S29.

Please cite this article in press as: Yadav et al., Techno-economic analysis and life cycle assessment for the catalytic hydrogenolysis and hydrocracking of polyethylene, Joule (2026), https://doi.org/10.1016/j.joule.2026.102384

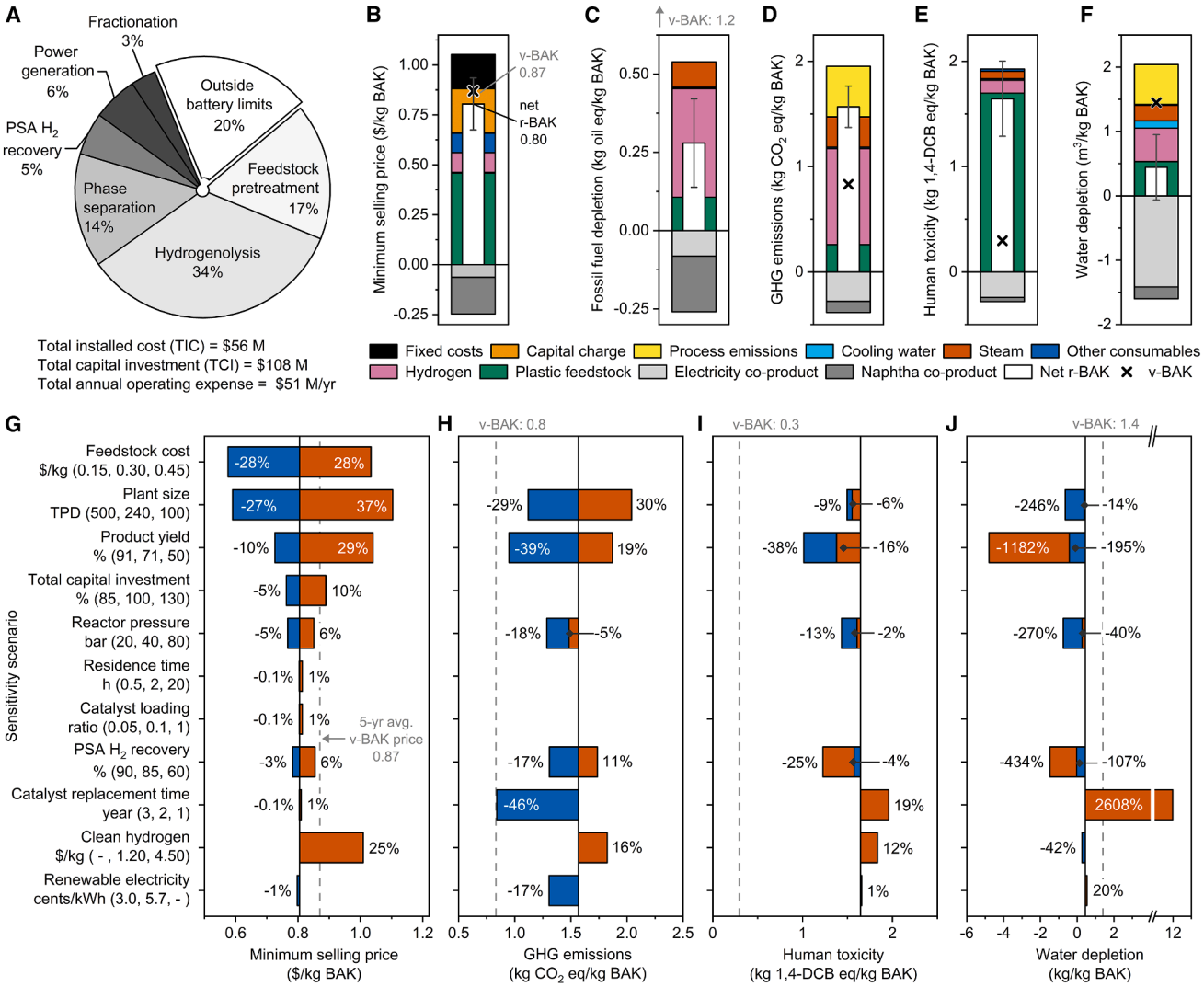

Figure 4. TEA, LCA, and sensitivity analysis results for case B (r-BAK product)

(A) Capital cost breakdown by area for each process section for case B, with TCI of $108 M. The TIC is split into different steps of the recycling process, including OSBL, which is assumed to be 25% of the battery limit investment.

(B) The MSP of the product. The net value is shown as a white bar, with the contribution breakdown shown behind the net value as colored segments. The 5-year average market price for v-BAK is shown for reference as a black "x". Error bars showing the standard deviation were estimated from a Monte Carlo analysis with 10,000 runs.

(C–F) Results for (C) fossil fuel depletion, (D) GHG emissions, (E) human toxicity, and (F) water depletion for the process. The net value and contributions are shown in a similar manner to the MSP.

(G–J) The effect of sensitivity cases on (G), MSP (H) GHG emissions, (I) human toxicity, and (J) water depletion. Blue and orange bars indicate the optimistic and pessimistic sensitivity cases, respectively, corresponding to the values in the y-axis labels.

LCA calculations were conducted with IPCC 2021 and ReCiPe methodologies, Brightway software, and ecoinvent 3.9.1 background data. Data for this figure are available in Tables S22–S28.

The r-BAK scenario is also estimated to have lower freshwater eutrophication, fossil fuel depletion, ionizing radiation, land use, metal depletion, ozone depletion, particulate matter formation, photo-oxidant formation, terrestrial acidification, and water depletion than v-BAK (Figures 4C–4F; Tables S19, S28, and S29). However, GHG emissions, ecotoxicity, marine eutrophication, and human toxicity of r-BAK are estimated to be 88%, 10%, 76%, and 5 times higher, respectively, than v-BAK. The overall impacts of r-BAK tend to be slightly lower than r-LSRN. The higher yields of r-BAK (71%) in comparison with r-LSRN (44%) and lower H_2 demand (0.08 kg/kg r-BAK vs. 0.13 kg/kg r-LSRN) counteract the fact that less electricity is co-generated due to higher energy demands for the 40-bar reactor and downstream separations (0.59 kWh/kg r-BAK vs. 1.40 kWh/kg r-LSRN). Across all r-BAK life cycle metrics, plastic collection and sortation contribute 13%–95%, H_2 accounts for 1%–64%,

Please cite this article in press as: Yadav et al., Techno-economic analysis and life cycle assessment for the catalytic hydrogenolysis and hydrocracking of polyethylene, Joule (2026), https://doi.org/10.1016/j.joule.2026.102384

and steam contributes 2%–42% for the same reasons outlined above for the r-LSRN scenario. The release of 0.48 kg CO_2 from combustion of the fuel co-product to generate electricity also accounts for 25% of GHG emissions.

The TEA and LCA sensitivity analyses (Figures 4G–4J; Tables S27 and S29) show the same trends as in the case of r-LSRN. One exception is that the low-yield case moderately improves the life cycle performance of r-BAK for select metrics. A 50% yield increases the co-generated electricity to 3.3 kWh/kg r-BAK, compared with 0.59 kWh in the base case, counteracting the environmental burdens of increased feedstock and consumable demand. This scenario, as well as the H_2 recovery sensitivity discussed above for r-LSRN, highlights that a single technical change can, in some cases, affect multiple parameters and complicate linear prediction of trends.

In general, BAK products are more economically valuable than LSRN products due to their higher octane ratings, making them a more suitable blendstock for conventional gasoline. Based on this result, we investigated the possibility of directly blending the r-BAK product into an existing refinery stream to generate economic benefits for petroleum refiners (see supplemental information for details). Using AspenTech's process industry modeling system (PIMS) software, the evaluation aimed to maximize refinery gross margin under constraints on crude availability, process unit capacities, and fuel specifications. The r-BAK blending properties were sourced from literature and Aspen Plus simulations.[95] Offered at fixed volumes of 5,000–30,000 barrels/day, the PIMS optimizer determined the best gasoline blending pool based on price and properties. The break-even value (BEV), the maximum cost refiners would pay to maintain gross margin without the blendstock, was used as a valuation metric. Input variables reflected varying economic conditions, including West Texas Intermediate (WTI) crude prices and demand projections from Energy Information Adminstration's annual energy outlook. BEVs increased with higher crude prices but decreased with higher purchase volumes due to necessary operational shifts in refinery units, reducing profitability (Figures S11 and S12). BEV also declined over time, significantly dropping by 2050 under a net-zero GHG emissions scenario, reflecting reduced gasoline demand. The results suggest r-BAK could be competitively priced with fossil-derived alkylate if produced in sufficient quantities, but low crude prices and declining gasoline demand pose long-term economic risks.

Alkanes for chemicals

In this case, we modeled the commercial CATOFIN process for the conversion of propane and butane obtained from the hydrocracking of the PE feedstock, along with a recycling stream from other process sections to recover high-purity propylene and butenes/*iso*-butenes.[96,97] This process was modeled to reflect closed-loop recycling.

Case C: r-propylene product

Whereas the previous cases targeted liquid-range alkane products, here, light gas production is desired. The reaction was reported by Lee et al.[57] in a batch reactor study to convert PE at T_{rxn} = 375°C and P_{rxn} = 100 bar H_2 (45 bar H_2 filling pressure, scaled by reaction temperature) into a propane- (~50 wt %) and butane-rich (~23 wt %) gaseous stream along with other products, primarily <C12. This is accomplished with an H-ZSM-5 acid catalyst (Si/Al = 23).[57] These conditions are used in the process model, assuming the process reactor can achieve the reported alkane yields. The C3 and C4 alkanes are separated by a depropanizer column to yield C3 and C4 streams, which serve as feeds to the propane dehydrogenation (PDH) reactor and butane dehydrogenation reactor (BDH), respectively. The PDH reactor achieves a high single-pass conversion of 45% and the BDH reactor achieves 53% single-pass conversion for butane/*iso*-butane, with selectivity exceeding 88 wt % for propane and over 89 wt % for butane and *iso*-butane, effectively minimizing byproduct formation.[98] To boost conversion and product formation, the outlet streams from both reactors were recycled back after separation from their olefinic counterpart, as illustrated in Figure 5. The methodology is provided in the SI to recover polymer-grade (>99.5% purity) propylene and butenes.

The TCI of a PE hydrocracking plant that produces propylene as the principal product is projected to be $194 M (Figure 6A). The highest contribution (~30%) to the TCI for this plant is from the hydrocracking section, owing to the hydrocracker and H_2 compressors, with its high operating pressure (~100 bar) requiring more robust equipment design and thicker-walled vessels, thereby increasing the installation factor. As with other cases, a 25% contribution is assumed from the OSBL investment. The total annual operating expense of such a plant is $62 M (Figure S13). The co-products, including butenes, naphtha, and fuel gas, reduce the MSP of r-propylene to $0.84/kg (Figure 6B), which is lower than the price of v-propylene at $0.95/kg. A summary of the results from this economic analysis is provided in Tables S30–S36.

The only primary product examined in this work estimated to have statistically equivalent GHG emissions to the fossil-based equivalent is r-propylene. It also exhibits lower fossil fuel depletion, photo-oxidant formation, water use, and terrestrial acidification than v-propylene, although the remaining impact categories are 40 to 3,000 times higher (Figures 6C–6F; Tables S19, S37, and S38; system boundary in Figure S14). Several factors contribute to these results: first, unlike the r-LSRN and r-BAK scenarios, no electricity is co-generated in the r-propylene case. Instead, credits are received for the C2 and C4 products (0.44 kg/kg r-propylene), naphtha (0.59 kg/kg r-propylene), and fuel gas (0.04 kg/kg r-propylene) co-products, but these co-products only majorly affect a handful of impact categories, such as GHG emissions and fossil fuel depletion. As an additional check, we compared co-product handling using mass allocation (Figure S15), which was consistent with the system expansion results for most metrics. Second, the pressure of the hydrogenation reactor (100 bar), additional dehydrogenation reactor, and downstream separations require substantial refrigeration and other electricity use (1.3 kWh/kg r-propylene), steam (2.0 kg/kg r-propylene), and H_2 (0.07 kg/kg r-propylene). Taken together, plastic collection and sortation contribute 11%–81% across all r-propylene life cycle metrics, electricity accounts for 12%–83%, steam contributes 2%–47%, and H_2 contributes 1%–34%. In contrast, producing 1 kg of propylene from fossil fuels uses 0.04 to 1 kWh of electricity, ~1.5 kg of steam, and no H_2, depending on the manufacturing route.[4]

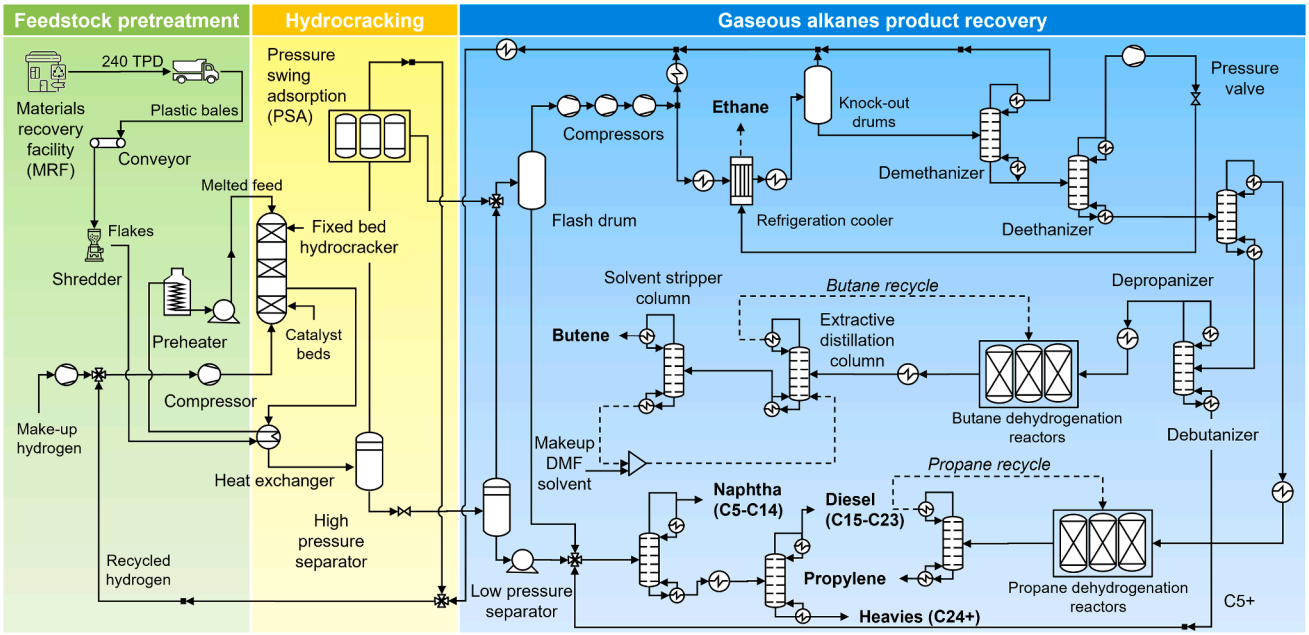

Figure 5. PFD for alkanes for chemical case

Simplified PFD of the polyolefin hydrocracking depolymerization process, divided into three sections. Feedstock pretreatment: In this section, polyolefin bales are debaled, flaked, and melted, and subsequently catalytically depolymerized in the next section. Hydrocracking: Following pretreatment, polymer flakes are catalytically cracked in the presence of hydrogen to generate a propane- and butane-rich stream. Product recovery: The hydrocracker effluent is cooled and separated to recover a H_2-rich gaseous stream, liquid alkanes, and an alkane-rich gas in a series of unit operations. The C3 and C4 alkanes are separated after passing through a series of refrigeration boxes. The PDH and BDH units are employed in parallel to convert propane and butane to their respective alkenes, and commercial refinery unit operations are used to recover polymer-grade products. Co-product credits are considered. The detailed PFD covering each process section of this base-case design is presented in Figures S3–S8 in supplemental information.

Univariate sensitivity analysis shows that the feedstock cost is the biggest driver for r-MSP, ranging from −46% to +45% (Figure 6G). Product yield is another major sensitivity parameter for both MSP and environmental impacts (Figures 6G–6J; Tables S36 and S38). In the base case, the total olefin yield was 74% (51% propylene and 23% butene). A 94% olefin yield reduces the MSP and environmental impacts of r-propylene by 5%–72%, whereas a 54% yield (41% propylene and 13% butene) leads to a 23%–192% increase. Economies of scale, including more efficient utility usage across a larger production volume, improve the product value and impact by 4%–39%. Enhancing H_2 recovery from 85% to 90% also decreases MSP and environmental impacts by 2%–18%. Note that water depletion in the base case is near zero due to co-product credits (−0.002 m^3/kg r-propylene) and is highly sensitive to any variations in electricity demand or co-product yield, hence the high percentage variations shown in Figure 6J. Additionally, less impactful sensitivity cases explored in this case study include varying the TCI, hydrogenolysis reactor pressure, residence time, and catalyst loading and replacement time. Furthermore, switching to clean H_2, decarbonized steam, and renewable electricity could decrease GHG emissions of r-propylene by 43%, 43%, and 48%, respectively. In contrast, switching to clean H_2 and decarbonized steam increases the MSP by 27% and 8%, respectively, and shifting to renewable electricity only enables a 4% reduction in MSP. Combining all these decarbonization pathways could allow r-propylene to exhibit net-negative emissions, well below the v-propylene benchmark of 1.5 kg CO_2e/kg.

DISCUSSION

Reductive catalytic depolymerization of polyolefins through hydrogenolysis and hydrocracking has re-emerged as a major area of interest in the recent wave of plastics chemical recycling research.[21–67] Given the magnitude of polyolefin production and the concomitant waste accumulation in landfills—over 31 M tons in 2019 in the US alone for PE and polypropylene[3]—these materials represent massive carbon resources to target for enabling circular supply chains. This work investigated three common outcomes of reductive depolymerization of the most abundantly produced polyolefin, PE, namely production of linear or branched alkanes and light olefins. Perhaps unsurprisingly, the product value, product yield, and feedstock cost are major drivers of estimated process feasibility. Relative to primary production, PE-derived linear alkanes slated for fuels do not exhibit beneficial economics or GHG emissions, branched alkanes exhibit similar economics but higher GHG emissions, and light olefins are close to parity for both metrics (Figure 7). While these results clearly demonstrate that further innovation is needed to reduce the process cost and environmental impacts of hydrogenolytic polyolefin depolymerization, a comparison with a similar process modeling effort for plastics pyrolysis[17] reveals that all cases studied here exhibit considerably lower GHG emissions,

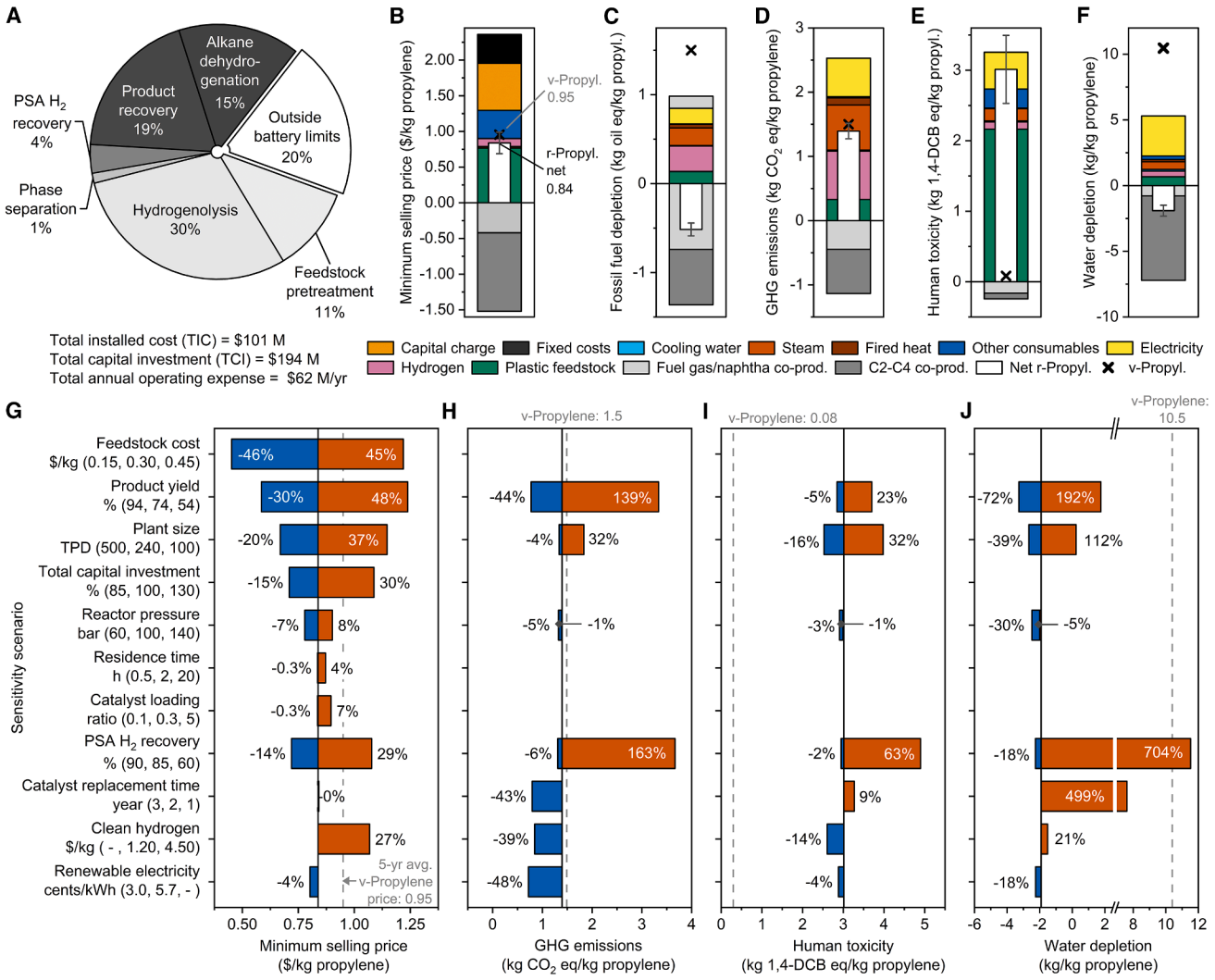

Figure 6. TEA, LCA, and sensitivity analysis results for case C (r-Propylene product)

(A) Capital cost breakdown by area for each process section for case C, with TCI of $194 M. The TIC is split into different steps of the recycling process, including OSBL, which is assumed to be 25% of the battery limit investment.

(B) The MSP of the product. The net value is shown as a white bar with the contribution breakdown shown behind the net value as colored segments. The 5-year average market price for v-propylene is shown for reference as a black "x". Error bars showing the standard deviation were estimated from a Monte Carlo analysis with 10,000 runs. The historical prices of products and co-products relative to WTI crude oil are shown in Figure S16.

(C–F) Results for (C) fossil fuel depletion, (D) GHG emissions, (E) human toxicity, and (F) water depletion for the process. The net value and contributions are shown in a similar manner to the MSP.

(G–J) The effect of sensitivity cases on (G) MSP, (H) GHG emissions, (I) human toxicity, and (J) water depletion. Blue and orange bars indicate the optimistic and pessimistic sensitivity cases, respectively, corresponding to the values in the *y*-axis labels.

LCA calculations were conducted with IPCC 2021 and ReCiPe methodologies, Brightway software, and ecoinvent 3.9.1 background data. Data for this figure are available in Tables S19 and S35–S38.

and in the branched alkanes and olefins cases, improved relative economics.

Early-stage process modeling, TEA, and LCA can typically serve as a quantitative guide to impactful research opportunities.[71,72] For catalysis researchers, the work here shows that catalyst cost and loading over the range of material formulations studied do not play a major role in economics or most environmental impacts, assuming long-term stability is achievable (2 years). Catalyst composition and architecture clearly dictate product selectivity and product yield, both of which are major drivers of economics and environmental impacts. Notably, while catalyst formulation dictates yield and selectivity, which indirectly affect process viability, sensitivity analysis also reveals that reducing the cost of incoming plastic waste has the most pronounced effect on MSP across all three scenarios. Thus, sourcing of low-cost, low-quality, or contaminated plastics (e.g., through improved preprocessing or catalyst tolerance) together with catalyst innovations will be more impactful than further process improvements alone.

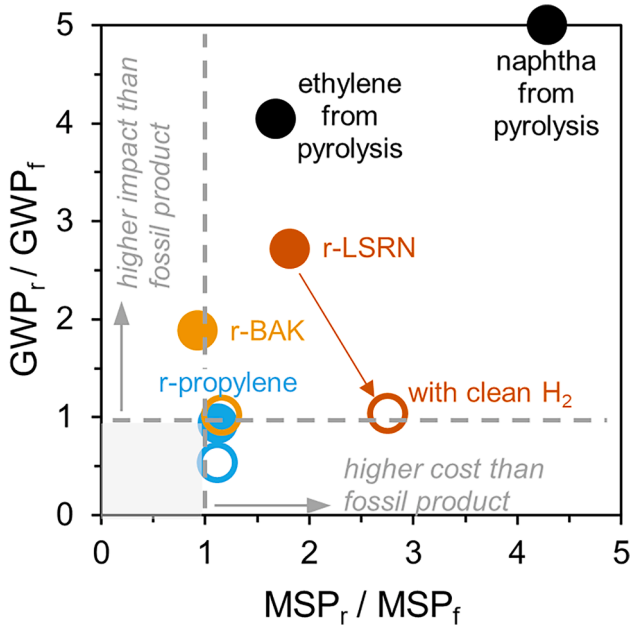

Figure 7. GHG emissions as a function of the minimum selling price (MSP) of all plastic hydrogenolysis case studies

Values are depicted as hydrogenolysis case GHG emissions (GHG_r) divided by the corresponding fossil fuel-based product GHG emissions (GHG_v) versus hydrogenolysis case MSP (MSP_r) divided by the corresponding fossil fuel-based MSP (MSP_v). Open circle points correspond to the clean H_2 scenario for each hydrogenolysis case. The points closest to the origin offer the most optimal combination of low GHGs and low MSP. Values for pyrolysis were obtained from the life cycle inventories in Yadav et al.,[17] updated to use consistent background data and LCA methods with those of this study.

Additionally, there are two previous process modeling studies of hydrogenolysis-based polyolefin that warrant comparison with this work. Cappello et al. modeled a process based on the Pt/$SrTiO_3$ catalyst from Celik et al.,[23] targeting production of polyalphaolefin lubricants.[99] Given the considerably higher value of lubricants relative to fuels, their study demonstrated advantageous economics, energy use, and GHG emissions relative to primary production. In a separate study, Hernández et al. compared multiple strategies for LDPE deconstruction, including hydrogenolysis and hydrocracking.[37] Similarly, they also noted that hydrogenolysis to produce mixed alkanes was economically viable when producing high-value lubricants, whereas hydrocracking to produce gasoline was not. While the results from both previous studies are promising for lubricant production, for open-loop processes such as reductive polyolefin depolymerization, it is important to consider the scale of feedstock and target product—globally, high-value lubricants are produced at two orders of magnitude less volume than the polyolefin waste volume in the US alone.

Overall, the results from this work highlight the challenge in producing fuel products that are both economically advantaged and exhibit lower environmental impacts than primary production. Notably, here we did not consider expanded system boundaries to address the life cycle impacts of fuel production from plastics, which we will consider in future work. From a research perspective, for closed-loop recycling applications back to polyolefins via monomer production, this work makes it clear that product yield, selectivity, and H_2 demand merit further attention to enable hydrogenolysis and hydrocracking processes to operate at scale. The identification of specific barriers toward scalability elucidates critical areas of technological innovation that have the potential to make this technology feasible, including catalyst development to improve product selectivity, reduction of hydrogen pressure demands, and operation with low-cost/low-quality plastic feedstocks.

METHODS

Methods are described throughout the main text, and further details can be found in the supplemental methods.

RESOURCE AVAILABILITY

Lead contact

Further information and requests for resources should be directed to and will be fulfilled by the lead contact, Gregg Beckham (gregg.beckham@nlr.gov).

Materials availability

This study did not generate new unique materials.

Data and code availability

The datasets in this article are provided in full in the supplemental information. The Aspen Plus models can be replicated by the inputs shown in the detailed PFD in the supplemental information. The Aspen models will be made available upon request.

ACKNOWLEDGMENTS

Funding was provided by the US Department of Energy, Office of Energy Efficiency and Renewable Energy, Advanced Materials and Manufacturing Technologies Office (AMMTO), and Bioenergy Technologies Office (BETO). This work was performed as part of the Bio-Optimized Technologies to keep Thermoplastics out of Landfills and the Environment (BOTTLE) Consortium and was supported by AMMTO and BETO under contract DE-AC36-08GO28308 with the National Renewable Energy Laboratory (NREL), operated by Alliance for Sustainable Energy, LLC. The BOTTLE Consortium includes members from MIT, funded under contract DE-AC36-08GO28308 with NREL. We thank Avantika Singh for helpful discussions. The views expressed in the article do not necessarily represent the views of the DOE or the US Government.

AUTHOR CONTRIBUTIONS

G.Y. developed the process and economic models with design input from T.U., J.S.D., J.E.R., and G.T.B. T.U. and E.C.V.R. conducted life cycle assessments. J.S.D., J.E.R., A.E.B., G.D., and G.Z. helped with model inputs, formal analysis, and data curation. G.Y., T.U., J.S.D., and E.C.V.R. made the figures. N.C. conducted the PIMS analysis for product blending with refinery streams. G.Y., T.U., J.S.D., Y.R.-L., and G.T.B. wrote the manuscript with contributions from all authors.

DECLARATION OF INTERESTS

J.E.R., A.E.B., G.D., G.Z., Y.R.-L., and G.T.B. have filed patent applications on reductive polyolefin depolymerization. G.T.B. is a member of the Recycling Science Council and an advisor to Entzimatiko, Samsara Eco, and Tereform.

SUPPLEMENTAL INFORMATION

Supplemental information can be found online at https://doi.org/10.1016/j.joule.2026.102384.

Received: August 10, 2025
Revised: November 14, 2025
Accepted: February 18, 2026

REFERENCES

1. Geyer, R., Jambeck, J.R., and Law, K.L. (2017). Production, use, and fate of all plastics ever made. Sci. Adv. *3*, e1700782. https://doi.org/10.1126/sciadv.1700782.
2. Nicholson, S.R., Rorrer, N.A., Carpenter, A.C., and Beckham, G.T. (2021). Manufacturing energy and greenhouse gas emissions associated with plastics consumption. Joule *5*, 673–686. https://doi.org/10.1016/j.joule.2020.12.027.
3. Milbrandt, A., Coney, K., Badgett, A., and Beckham, G.T. (2022). Quantification and evaluation of plastic waste in the United States. Resour. Conserv. Recycl. *183*, 106363. https://doi.org/10.1016/j.resconrec.2022.106363.
4. Nicholson, S.R., Rorrer, N.A., Uekert, T., Avery, G., Carpenter, A.C., and Beckham, G.T. (2023). Manufacturing energy and greenhouse gas emissions associated with United States consumption of organic petrochemicals. ACS Sustainable Chem. Eng. *11*, 2198–2208. https://doi.org/10.1021/acssuschemeng.2c05417.
5. Borrelle, S.B., Ringma, J., Law, K.L., Monnahan, C.C., Lebreton, L., McGivern, A., Murphy, E., Jambeck, J., Leonard, G.H., Hilleary, M.A., et al. (2020). Predicted growth in plastic waste exceeds efforts to mitigate plastic pollution. Science *369*, 1515–1518. https://doi.org/10.1126/science.aba3656.
6. Law, K.L., Starr, N., Siegler, T.R., Jambeck, J.R., Mallos, N.J., and Leonard, G.H. (2020). The United States' contribution of plastic waste to land and ocean. Sci. Adv. *6*, eabd0288. https://doi.org/10.1126/sciadv.abd0288.
7. Ragaert, K., Delva, L., and Van Geem, K. (2017). Mechanical and chemical recycling of solid plastic waste. Waste Manag. *69*, 24–58. https://doi.org/10.1016/j.wasman.2017.07.044.
8. Rahimi, A., and García, J.M. (2017). Chemical recycling of waste plastics for new materials production. Nat. Rev. Chem. *1*. https://doi.org/10.1038/s41570-017-0046.
9. Vollmer, I., Jenks, M.J.F., Roelands, M.C.P., White, R.J., Van Harmelen, T., De Wild, P., van Der Laan, G.P., Meirer, F., Keurentjes, J.T.F., and Weckhuysen, B.M. (2020). Beyond mechanical recycling: giving new life to plastic waste. Angew. Chem. Int. Ed. Engl. *59*, 15402–15423. https://doi.org/10.1002/anie.201915651.
10. Ellis, L.D., Rorrer, N.A., Sullivan, K.P., Otto, M., McGeehan, J.E., Román-Leshkov, Y., Wierckx, N., and Beckham, G.T. (2021). Chemical and biological catalysis for plastics recycling and upcycling. Nat. Catal. *4*, 539–556. https://doi.org/10.1038/s41929-021-00648-4.
11. Korley, L.T.J., Epps, T.H., III, Helms, B.A., and Ryan, A.J. (2021). Toward polymer upcycling—adding value and tackling circularity. Science *373*, 66–69. https://doi.org/10.1126/science.abg4503.
12. Martín, A.J., Mondelli, C., Jaydev, S.D., and Pérez-Ramírez, J. (2021). Catalytic processing of plastic waste on the rise. Chem *7*, 1487–1533. https://doi.org/10.1016/j.chempr.2020.12.006.
13. Jehanno, C., Alty, J.W., Roosen, M., De Meester, S., Dove, A.P., Chen, E.Y.-X., Leibfarth, F.A., and Sardon, H. (2022). Critical advances and future opportunities in upcycling commodity polymers. Nature *603*, 803–814. https://doi.org/10.1038/s41586-021-04350-0.
14. Sun, J., Dong, J., Gao, L., Zhao, Y.-Q., Moon, H., and Scott, S.L. (2024). Catalytic upcycling of polyolefins. Chem. Rev. *124*, 9457–9579. https://doi.org/10.1021/acs.chemrev.3c00943.
15. Vidal, F., van der Marel, E.R., Kerr, R.W.F., McElroy, C., Schroeder, N., Mitchell, C., Rosetto, G., Chen, T.T.D., Bailey, R.M., Hepburn, C., et al. (2024). Designing a circular carbon and plastics economy for a sustainable future. Nature *626*, 45–57. https://doi.org/10.1038/s41586-023-06939-z.
16. Afzal, S., Singh, A., Nicholson, S.R., Uekert, T., DesVeaux, J.S., Tan, E.C.D., Dutta, A., Carpenter, A.C., Baldwin, R.M., and Beckham, G.T. (2023). Techno-economic analysis and life cycle assessment of mixed plastic waste gasification for production of methanol and hydrogen. Green Chem. *25*, 5068–5085. https://doi.org/10.1039/D3GC00679D.
17. Yadav, G., Singh, A., Dutta, A., Uekert, T., DesVeaux, J.S., Nicholson, S.R., Tan, E.C.D., Mukarakate, C., Schaidle, J.A., Wrasman, C.J., et al. (2023). Techno-economic analysis and life cycle assessment for catalytic fast pyrolysis of mixed plastic waste. Energy Environ. Sci. *16*, 3638–3653. https://doi.org/10.1039/D3EE00749A.
18. Chu, M., Liu, Y., Lou, X., Zhang, Q., and Chen, J. (2022). Rational design of chemical catalysis for plastic recycling. ACS Catal. *12*, 4659–4679. https://doi.org/10.1021/acscatal.2c01286.
19. Dong, Z., Chen, W., Xu, K., Liu, Y., Wu, J., and Zhang, F. (2022). Understanding the structure–activity relationships in catalytic conversion of polyolefin plastics by zeolite-based catalysts: A critical review. ACS Catal. *12*, 14882–14901. https://doi.org/10.1021/acscatal.2c04915.
20. Hinton, Z.R., Talley, M.R., Kots, P.A., Le, A.V., Zhang, T., Mackay, M.E., Kunjapur, A.M., Bai, P., Vlachos, D.G., Watson, M.P., et al. (2022). Innovations toward the valorization of plastics waste. Annu. Rev. Mater. Res. *52*, 249–280. https://doi.org/10.1146/annurev-matsci-081320-032344.
21. Kots, P.A., Vance, B.C., and Vlachos, D.G. (2022). Polyolefin plastic waste hydroconversion to fuels, lubricants, and waxes: a comparative study. React. Chem. Eng. *7*, 41–54. https://doi.org/10.1039/D1RE00447F.
22. Dufaud, V., and Basset, J.M. (1998). Catalytic hydrogenolysis at low temperature and pressure of polyethylene and polypropylene to diesels or lower alkanes by a zirconium hydride supported on silica-alumina: a step toward polyolefin degradation by the microscopic reverse of ziegler–natta polymerization. Angew. Chem. Int. Ed. *37*, 806–810. https://doi.org/10.1002/(SICI)1521-3773(19980403)37:6<806::AID-ANIE806>3.0.CO;2-6.
23. Celik, G., Kennedy, R.M., Hackler, R.A., Ferrandon, M., Tennakoon, A., Patnaik, S., LaPointe, A.M., Ammal, S.C., Heyden, A., Perras, F.A., et al. (2019). Upcycling single-use polyethylene into high-quality liquid products. ACS Cent. Sci. *5*, 1795–1803. https://doi.org/10.1021/acscentsci.9b00722.
24. Tennakoon, A., Wu, X., Paterson, A.L., Patnaik, S., Pei, Y., LaPointe, A.M., Ammal, S.C., Hackler, R.A., Heyden, A., Slowing, I.I., et al. (2020). Catalytic upcycling of high-density polyethylene via a processive mechanism. Nat. Catal. *3*, 893–901. https://doi.org/10.1038/s41929-020-00519-4.
25. Zhang, F., Zeng, M., Yappert, R.D., Sun, J., Lee, Y.-H., LaPointe, A.M., Peters, B., Abu-Omar, M.M., and Scott, S.L. (2020). Polyethylene upcycling to long-chain alkylaromatics by tandem hydrogenolysis/aromatization. Science *370*, 437–441. https://doi.org/10.1126/science.abc5441.
26. Jaydev, S.D., Martín, A.J., and Pérez-Ramírez, J. (2021). Direct conversion of polypropylene into liquid hydrocarbons on carbon-supported platinum catalysts. ChemSusChem *14*, 5179–5185. https://doi.org/10.1002/cssc.202101999.
27. Jia, C., Xie, S., Zhang, W., Intan, N.N., Sampath, J., Pfaendtner, J., and Lin, H. (2021). Deconstruction of high-density polyethylene into liquid hydrocarbon fuels and lubricants by hydrogenolysis over Ru catalyst. Chem. Catal. *1*, 437–455. https://doi.org/10.1016/j.checat.2021.04.002.
28. Kots, P.A., Liu, S., Vance, B.C., Wang, C., Sheehan, J.D., and Vlachos, D.G. (2021). Polypropylene plastic waste conversion to lubricants over Ru/TiO_2 catalysts. ACS Catal. *11*, 8104–8115. https://doi.org/10.1021/acscatal.1c00874.

29. Nakaji, Y., Tamura, M., Miyaoka, S., Kumagai, S., Tanji, M., Nakagawa, Y., Yoshioka, T., and Tomishige, K. (2021). Low-temperature catalytic upgrading of waste polyolefinic plastics into liquid fuels and waxes. Appl. Catal. B: Environ. Energy *285*, 119805. https://doi.org/10.1016/j.apcatb.2020.119805.

30. Rorrer, J.E., Beckham, G.T., and Román-Leshkov, Y. (2021). Conversion of polyolefin waste to liquid alkanes with Ru-based catalysts under mild conditions. JACS Au *1*, 8–12. https://doi.org/10.1021/jacsau.0c00041.

31. Borkar, S.S., Helmer, R., Mahnaz, F., Majzoub, W., Mahmoud, W., Al-Rawashdeh, M., and Shetty, M. (2022). Enabling resource circularity through thermo-catalytic and solvent-based conversion of waste plastics. Chem. Catal. *2*, 3320–3356. https://doi.org/10.1016/j.checat.2022.09.003.

32. Chen, L., Meyer, L.C., Kovarik, L., Meira, D., Pereira-Hernandez, X.I., Shi, H., Khivantsev, K., Gutiérrez, O.Y., and Szanyi, J. (2022). Disordered, sub-nanometer Ru structures on CeO2 are highly efficient and selective catalysts in polymer upcycling by hydrogenolysis. ACS Catal. *12*, 4618–4627. https://doi.org/10.1021/acscatal.2c00684.

33. Tamura, M., Miyaoka, S., Nakaji, Y., Tanji, M., Kumagai, S., Nakagawa, Y., Yoshioka, T., and Tomishige, K. (2022). Structure-activity relationship in hydrogenolysis of polyolefins over Ru/support catalysts. Appl. Catal. B: Environ. Energy *318*, 121870. https://doi.org/10.1016/j.apcatb.2022.121870.

34. Wu, X., Tennakoon, A., Yappert, R., Esveld, M., Ferrandon, M.S., Hackler, R.A., LaPointe, A.M., Heyden, A., Delferro, M., Peters, B., et al. (2022). Size-Controlled Nanoparticles Embedded in a Mesoporous Architecture Leading to Efficient and Selective Hydrogenolysis of Polyolefins. J. Am. Chem. Soc. *144*, 5323–5334. https://doi.org/10.1021/jacs.1c11694.

35. Chen, S., Tennakoon, A., You, K.-E., Paterson, A.L., Yappert, R., Alayoglu, S., Fang, L., Wu, X., Zhao, T.Y., Lapak, M.P., et al. (2023). Ultrasmall amorphous zirconia nanoparticles catalyse polyolefin hydrogenolysis. Nat. Catal. *6*, 161–173. https://doi.org/10.1038/s41929-023-00910-x.

36. Hancock, J.N., and Rorrer, J.E. (2023). Hydrogen-free catalytic depolymerization of waste polyolefins at mild temperatures. Appl. Catal. B: Environ. Energy *338*, 123071. https://doi.org/10.1016/j.apcatb.2023.123071.

37. Hernández, B., Kots, P., Selvam, E., Vlachos, D.G., and Ierapetritou, M.G. (2023). Techno-economic and life cycle analyses of thermochemical upcycling technologies of low-density polyethylene waste. ACS Sustainable Chem. Eng. *11*, 7170–7181. https://doi.org/10.1021/acssuschemeng.3c00636.

38. Jaydev, S.D., Usteri, M.-E., Martín, A.J., and Pérez-Ramírez, J. (2023). Identifying selective catalysts in polypropylene hydrogenolysis by decoupling scission pathways. Chem. Catal. *3*, 100564. https://doi.org/10.1016/j.checat.2023.100564.

39. Tennakoon, A., Wu, X., Meirow, M., Howell, D., Willmon, J., Yu, J., Lamb, J.V., Delferro, M., Luijten, E., Huang, W., and Sadow, A.D. (2023). Two Mesoporous Domains Are Better Than One for Catalytic Deconstruction of Polyolefins. J. Am. Chem. Soc. *145*, 17936–17944. https://doi.org/10.1021/jacs.3c05447.

40. Vance, B.C., Kots, P.A., Wang, C., Granite, J.E., and Vlachos, D.G. (2023). Ni/SiO2 catalysts for polyolefin deconstruction via the divergent hydrogenolysis mechanism. Appl. Catal. B: Environ. Energy *322*, 122138. https://doi.org/10.1016/j.apcatb.2022.122138.

41. Wang, H., Yoskamtorn, T., Zheng, J., Ho, P.-L., Ng, B., and Tsang, S.C.E. (2023). Ce-Promoted PtSn-Based Catalyst for Hydrocracking of Polyolefin Plastic Waste into High Yield of Gasoline-Range Products. ACS Catal. *13*, 15886–15898. https://doi.org/10.1021/acscatal.3c03996.

42. Zhang, W., Kim, S., Wahl, L., Khare, R., Hale, L., Hu, J., Camaioni, D.M., Gutiérrez, O.Y., Liu, Y., and Lercher, J.A. (2023). Low-temperature upcycling of polyolefins into liquid alkanes via tandem cracking-alkylation. Science *379*, 807–811. https://doi.org/10.1126/science.ade7485.

43. Hu, Q., Qian, S., Wang, Y., Zhao, J., Jiang, M., Sun, M., Huang, H., Gan, T., Ma, J., Zhang, J., et al. (2024). Polyethylene hydrogenolysis by dilute RuPt alloy to achieve H2-pressure-independent low methane selectivity. Nat. Commun. *15*, 10573. https://doi.org/10.1038/s41467-024-54786-x.

44. Jaydev, S.D., Martín, A.J., Garcia, D., Chikri, K., and Pérez-Ramírez, J. (2024). Assessment of transport phenomena in catalyst effectiveness for chemical polyolefin recycling. Nat. Chem. Eng. *1*, 565–575. https://doi.org/10.1038/s44286-024-00108-3.

45. Wang, Y.-Y., Tennakoon, A., Wu, X., Sahasrabudhe, C., Qi, L., Peters, B.G., Sadow, A.D., and Huang, W. (2024). Catalytic hydrogenolysis of polyethylene under reactive separation. ACS Catal. *14*, 2084–2094. https://doi.org/10.1021/acscatal.3c04987.

46. Kim, S., Yang, B., Gutiérrez, O.Y., Zhang, W., Lizandara-Pueyo, C., Ingale, P., Jevtovikj, I., Grauke, R., Szanyi, J., Wang, H., et al. (2025). Ru-Catalyzed Polyethylene Hydrogenolysis under Quasi-Supercritical Conditions. JACS Au *5*, 1760–1770. https://doi.org/10.1021/jacsau.5c00006.

47. Chu, M., Wang, X., Wang, X., Lou, X., Zhang, C., Cao, M., Wang, L., Li, Y., Liu, S., Sham, T.-K., et al. (2023). Site-Selective Polyolefin Hydrogenolysis on Atomic Ru for Methanation Suppression and Liquid Fuel Production. Research (Wash D. C) *6*, 0032. https://doi.org/10.34133/research.0032.

48. Ji, H., Wang, X., Wei, X., Peng, Y., Zhang, S., Song, S., and Zhang, H. (2023). Boosting Polyethylene Hydrogenolysis Performance of Ru-CeO2 Catalysts by Finely Regulating the Ru Sizes. Small *19*, e2300903. https://doi.org/10.1002/smll.202300903.

49. Meirow, M., Tennakoon, A., Wu, X., Willmon, J., Howell, D., Huang, W., Sadow, A.D., and Luijten, E. (2023). Influence of Pore Length on Hydrogenolysis of Polyethylene within a Mesoporous Support Architecture. J. Phys. Chem. C *127*, 23805–23813. https://doi.org/10.1021/acs.jpcc.3c04300.

50. Chu, M., Wang, X., Wang, X., Xu, P., Zhang, L., Li, S., Feng, K., Zhong, J., Wang, L., Li, Y., et al. (2024). Layered Double Hydroxide Derivatives for Polyolefin Upcycling. J. Am. Chem. Soc. *146*, 10655–10665. https://doi.org/10.1021/jacs.4c00327.

51. Kang, Q., Chu, M., Xu, P., Wang, X., Wang, S., Cao, M., Ivasenko, O., Sham, T.-K., Zhang, Q., Sun, Q., and Chen, J. (2023). Entropy Confinement Promotes Hydrogenolysis Activity for Polyethylene Upcycling. Angew. Chem. Int. Ed. Engl. *62*, e202313174. https://doi.org/10.1002/anie.202313174.

52. Pennel, M.L., Jiang, Y., and Cargnello, M. (2024). Influence of Autoclave Liner on Polyethylene Hydrogenolysis Selectivity. ACS Sustainable Resour. Manage. *1*, 1047–1052. https://doi.org/10.1021/acssusresmgt.4c00112.

53. Yuan, Y., Xie, Z., Turaczy, K.K., Hwang, S., Zhou, J., and Chen, J.G. (2024). Controlling Product Distribution of Polyethylene Hydrogenolysis Using Bimetallic RuM3 (M = Fe, Co, Ni) Catalysts. Chem. Bio Eng. *1*, 67–75. https://doi.org/10.1021/cbe.3c00007.

54. Bin Jumah, A., Anbumuthu, V., Tedstone, A.A., and Garforth, A.A. (2019). Catalyzing the Hydrocracking of Low Density Polyethylene. Ind. Eng. Chem. Res. *58*, 20601–20609. https://doi.org/10.1021/acs.iecr.9b04263.

55. Vance, B.C., Kots, P.A., Wang, C., Hinton, Z.R., Quinn, C.M., Epps, T.H., Korley, L.T.J., and Vlachos, D.G. (2021). Single pot catalyst strategy to branched products via adhesive isomerization and hydrocracking of polyethylene over platinum tungstated zirconia. Appl. Catal. B: Environ. Energy *299*, 120483. https://doi.org/10.1016/j.apcatb.2021.120483.

56. Duan, J., Chen, W., Wang, C., Wang, L., Liu, Z., Yi, X., Fang, W., Wang, H., Wei, H., Xu, S., et al. (2022). Coking-Resistant Polyethylene Upcycling Modulated by Zeolite Micropore Diffusion. J. Am. Chem. Soc. *144*, 14269–14277. https://doi.org/10.1021/jacs.2c05125.

57. Lee, W.-T., van Muyden, A., Bobbink, F.D., Mensi, M.D., Carullo, J.R., and Dyson, P.J. (2022). Mechanistic classification and benchmarking of polyolefin depolymerization over silica-alumina-based catalysts. Nat. Commun. *13*, 4850. https://doi.org/10.1038/s41467-022-32563-y.

58. Rorrer, J.E., Ebrahim, A.M., Questell-Santiago, Y., Zhu, J., Troyano-Valls, C., Asundi, A.S., Brenner, A.E., Bare, S.R., Tassone, C.J., Beckham, G.T., and Román-Leshkov, Y. (2022). Role of Bifunctional Ru/Acid Catalysts in

the Selective Hydrocracking of Polyethylene and Polypropylene Waste to Liquid Hydrocarbons. ACS Catal. *12*, 13969–13979. https://doi.org/10.1021/acscatal.2c03596.

59. Liu, S., Kots, P.A., Vance, B.C., Danielson, A., and Vlachos, D.G. (2021). Plastic waste to fuels by hydrocracking at mild conditions. Sci. Adv. *7*, eabf8283. https://doi.org/10.1126/sciadv.abf8283.
60. Wang, C., Xie, T., Kots, P.A., Vance, B.C., Yu, K., Kumar, P., Fu, J., Liu, S., Tsilomelekis, G., Stach, E.A., et al. (2021). Polyethylene Hydrogenolysis at Mild Conditions over Ruthenium on Tungstated Zirconia. JACS Au *1*, 1422–1434. https://doi.org/10.1021/jacsau.1c00200.
61. Chen, L., Moreira, J.B., Meyer, L.C., and Szanyi, J. (2023). Efficient and selective dual-pathway polyolefin hydro-conversion over unexpectedly bifunctional M/TiO2-anatase catalysts. Appl. Catal. B: Environ. Energy *335*, 122897. https://doi.org/10.1016/j.apcatb.2023.122897.
62. Kots, P.A., Doika, P.A., Vance, B.C., Najmi, S., and Vlachos, D.G. (2023). Tuning High-Density Polyethylene Hydrocracking through Mordenite Zeolite Crystal Engineering. ACS Sustainable Chem. Eng. *11*, 9000–9009. https://doi.org/10.1021/acssuschemeng.3c01515.
63. Qiu, Z., Lin, S., Chen, Z., Chen, A., Zhou, Y., Cao, X., Wang, Y., and Lin, B.-L. (2023). A reusable, impurity-tolerant and noble metal–free catalyst for hydrocracking of waste polyolefins. Sci. Adv. *9*, eadg5332. https://doi.org/10.1126/sciadv.adg5332.
64. Tan, J.Z., Hullfish, C.W., Zheng, Y., Koel, B.E., and Sarazen, M.L. (2023). Conversion of polyethylene waste to short chain hydrocarbons under mild temperature and hydrogen pressure with metal-free and metal-loaded MFI zeolites. Appl. Catal. B: Environ. Energy *338*, 123028. https://doi.org/10.1016/j.apcatb.2023.123028.
65. Lamb, J.V., Lee, Y.-H., Sun, J., Byron, C., Uppuluri, R., Kennedy, R.M., Meng, C., Behera, R.K., Wang, Y.-Y., Qi, L., et al. (2024). Supported Platinum Nanoparticles Catalyzed Carbon–Carbon Bond Cleavage of Polyolefins: Role of the Oxide Support Acidity. ACS Appl. Mater. Interfaces *16*, 11361–11376. https://doi.org/10.1021/acsami.3c15350.
66. Liu, Y., Dai, W., Zheng, J., Du, Y., Wang, Q., Hedin, N., Qin, B., and Li, R. (2024). Selective and Controllable Cracking of Polyethylene Waste by Beta Zeolites with Different Mesoporosity and Crystallinity. Adv. Sci. (Weinh) *11*, e2404426. https://doi.org/10.1002/advs.202404426.
67. Zhao, P., Guo, W., Gui, Z., Jiang, J., Zhu, Z., Li, J.-J., Zhao, L., Zhou, J., and Xi, Z. (2024). Selective Hydrocracking of Waste Polyolefins toward Gasoline-Range Liquid Fuels via Tandem Catalysis over a Cerium-Promoted Pt/HY Catalyst. ACS Sustainable Chem. Eng. *12*, 5738–5752. https://doi.org/10.1021/acssuschemeng.3c04163.
68. Weitkamp, J. (2012). Catalytic Hydrocracking—Mechanisms and Versatility of the Process. ChemCatChem *4*, 292–306. https://doi.org/10.1002/cctc.201100315.
69. Tan, J.Z., Ortega, M., Miller, S.A., Hullfish, C.W., Kim, H., Kim, S., Hu, W., Hu, J.Z., Lercher, J.A., Koel, B.E., and Sarazen, M.L. (2024). Catalytic Consequences of Hierarchical Pore Architectures within MFI and FAU Zeolites for Polyethylene Conversion. ACS Catal. *14*, 7536–7552. https://doi.org/10.1021/acscatal.4c01213.
70. Zhou, X., Han, X., Qu, Z., Zhang, J., Zeng, F., Tang, Z., and Chen, R. (2024). Hierarchical FAU Zeolites Boosting the Hydrocracking of Polyolefin Waste into Liquid Fuels. ACS Sustainable Chem. Eng. *12*, 6013–6022. https://doi.org/10.1021/acssuschemeng.4c01097.
71. Nicholson, S.R., Rorrer, J.E., Singh, A., Konev, M.O., Rorrer, N.A., Carpenter, A.C., Jacobsen, A.J., Román-Leshkov, Y., and Beckham, G.T. (2022). The critical role of process analysis in chemical recycling and upcycling of waste plastics. Annu. Rev. Chem. Biomol. Eng. *13*, 301–324. https://doi.org/10.1146/annurev-chembioeng-100521-085846.
72. Nixon, K.D., Schyns, Z.O.G., Luo, Y., Ierapetritou, M.G., Vlachos, D.G., Korley, L.T.J., Epps, T.H., and Thomas, H. (2024). Analyses of circular solutions for advanced plastics waste recycling. Nat. Chem. Eng. *1*, 615–626. https://doi.org/10.1038/s44286-024-00121-6.
73. RecyclingMarkets.net. (2023). Secondary Materials Pricing. Recycling Markets. https://www.recyclingmarkets.net/index.php.
74. Amstar Machinery, Ltd. (2022). Single shaft shredder for PE films. https://www.plasticrecyclingmachine.net/.
75. Prasad, A. (1998). A quantitative analysis of low density polyethylene and linear low density polyethylene blends by differential scanning calorimetery and fourier transform infrared spectroscopy methods. Polymer Engineering & Sci. *38*, 1716–1728. https://doi.org/10.1002/pen.10342.
76. Gary, J.H., Handwerk, G.E., and Kaiser, M.J. (2007). Petroleum Refining: Technology and Economics (CRC Press).
77. Chou, T.-S., Kennedy, C.R., and Shih, S.S. (1991). Hydroconversion process. US patent 4997544. filed May 12, 1989, and granted March 5, 1991.
78. Baddour, F., Van Allsburg, K., Wunder, N., Yarbrough, J., Jankousky, M., Gruchalla, K., Potter, K., Schaidle, J., Tan, E., Talmadge, M., et al. (2019). CatCost^{TM} (Catalyst Cost Estimation Tool). https://ui.adsabs.harvard.edu/abs/2019doe..soft..130B/abstract.
79. Dutta, A., Sahir, A., Tan, E., Humbird, D., Snowden-Swan, L.J., Meyer, P.A., Ross, J., Sexton, D., Yap, R., and Lukas, J. (2015). Process design and economics for the conversion of lignocellulosic biomass to hydrocarbon fuels: Thermochemical research pathways with in situ and ex situ upgrading of fast pyrolysis vapors. Pacific Northwest National Lab.(PNNL). https://doi.org/10.2172/1215007.
80. Chang, R.J., and Lacson, J. (2021). Process Economics Program (PEP) Yearbook Price History. https://www.spglobal.com/energy/en/products-solutions/chemicals/chemical-process-economics-program-pep.
81. Wernet, G., Bauer, C., Steubing, B., Reinhard, J., Moreno-Ruiz, E., and Weidema, B. (2016). The ecoinvent database version 3 (part I): overview and methodology. Int. J. Life Cycle Assess. *21*, 1218–1230. https://doi.org/10.1007/s11367-016-1087-8.
82. Intergovernmental Panel on Climate. (2023). Climate Change 2021 – The Physical Science Basis: Working Group I Contribution to the Sixth Assessment Report of the Intergovernmental Panel on Climate Change (Cambridge University Press). https://doi.org/10.1017/9781009157896.
83. Huijbregts, M.A.J., Steinmann, Z.J.N., Elshout, P.M.F., Stam, G., Verones, F., Vieira, M., Zijp, M., Hollander, A., and van Zelm, R. (2017). ReCiPe2016: a harmonised life cycle impact assessment method at midpoint and endpoint level. Int. J. Life Cycle Assess. *22*, 138–147. https://doi.org/10.1007/s11367-016-1246-y.
84. The Association of Plastic Recyclers. (2018). 2018 Life Cycle Impacts for Post-consumer Recycled Resins: PET, HDPE, and PP. https://plasticsrecycling.org/resources/2018-life-cycle-impacts-for-postconsumer-recycled-resins-pet-hdpe-pp/.
85. Muller, S., Lesage, P., Ciroth, A., Mutel, C., Weidema, B.P., and Samson, R. (2016). The application of the pedigree approach to the distributions foreseen in ecoinvent v3. Int. J. Life Cycle Assess. *21*, 1327–1337. https://doi.org/10.1007/s11367-014-0759-5.
86. DeCarolis, J., and LaRose, A. (2023). Annual Energy Outlook 2023 (US Energy Information Administration).
87. Ghosh, T., Avery, G., Bhatt, A., Uekert, T., Walzberg, J., and Carpenter, A. (2023). Towards a circular economy for PET bottle resin using a system dynamics inspired material flow model. J. Clean. Prod. *383*, 135208. https://doi.org/10.1016/j.jclepro.2022.135208.
88. Victor, N., and Nichols, C. (2024). Future of hydrogen in the U.S. energy sector: MARKAL modeling results. Appl. Energy Combust. Sci. *18*, 100259. https://doi.org/10.1016/j.jaecs.2024.100259.
89. Sun, P., Young, B., Elgowainy, A., Lu, Z., Wang, M., Morelli, B., and Hawkins, T. (2019). Criteria Air Pollutants and Greenhouse Gas Emissions from Hydrogen Production in U.S. Steam Methane Reforming Facilities. Environ. Sci. Technol. *53*, 7103–7113. https://doi.org/10.1021/acs.est.8b06197.
90. Cho, H.H., Strezov, V., and Evans, T.J. (2022). Environmental impact assessment of hydrogen production via steam methane reforming based

on emissions data. Energy Rep. *8*, 13585–13595. https://doi.org/10.1016/j.egyr.2022.10.053.

91. Ho, J., Becker, J., Brown, M., Brown, P., Chernyakhovskiy, I., Cohen, S., Cole, W., Corcoran, S., Eurek, K., Frazier, W., et al. (2021). Regional Energy Deployment System (ReEDS) Model Documentation (Version 2020). https://www.osti.gov/biblio/1788425.
92. James, B.D., Huya-Kouadio, J.M., Houchins, C., Acevedo, Y., and McNamara, K.R. (2021). H2 Production Pathways Cost Analysis (2016 - 2021). Final Report (Strategic Analysis Inc.). https://www.osti.gov/biblio/2280867.
93. ICF. (2020). Study on the Use of Biofuels (Renewable Natural Gas) in the Greater Washington, D.C. Metropolitan Area. https://www.worldbiogasassociation.org/wp-content/uploads/2020/03/200316-WGL-RNG-Report-FINAL-1.pdf.
94. Seel, J., Kemp, J.M., Cheyette, A., Millstein, D., Gorman, W., Jeong, S., Robson, D., Setiawan, R., and Bolinger, M. (2024). Utility-Scale Solar, 2024 Edition: Empirical Trends in Deployment, Technology, Cost,. Performance, PPA Pricing, and Valuein the United States (Lawrence Berkeley National Laboratory). https://emp.lbl.gov/sites/default/files/2024-10/Utility%20Scale%20Solar%202024%20Edition%20Slides.pdf.
95. Jiang, Y., Zaimes, G.G., Li, S., Hawkins, T.R., Singh, A., Carlson, N., Talmadge, M., Gaspar, D.J., Ramirez-Corredores, M.M., Beck, A.W., et al. (2023). Economic and environmental analysis to evaluate the potential value of co-optima diesel bioblendstocks to petroleum refiners. Fuel *333*, 126233. https://doi.org/10.1016/j.fuel.2022.126233.
96. Zimmermann, H., and Walzl, R. (2000). Ethylene. In Ullmann's Encyclopedia of Industrial Chemistry, C. Ley, ed. (Wiley-VCH Verlag GmbH & Company. KGaA). https://doi.org/10.1002/14356007.a10_045.pub3.
97. Meyers, R.A. (2004). Handbook of Petroleum Refining Processes (McGraw Hill).
98. LummusTechnology. (2023). CATOFIN® Propane/Butane Dehydrogenation. https://www.lummustechnology.com/process-technologies/petrochemicals/butadiene-butylene-production/propane-butane-dehydrogenation.
99. Cappello, V., Sun, P., Zang, G., Kumar, S., Hackler, R., Delgado, H.E., Elgowainy, A., Delferro, M., and Krause, T. (2022). Conversion of plastic waste into high-value lubricants: techno-economic analysis and life cycle assessment. Green Chem. *24*, 6306–6318. https://doi.org/10.1039/D2GC01840C.